AGU PUBLICATIONS

Geophysical Research Letters

RESEARCH LETTER
10.1002/2014GL060513

The 2010–2014.3 global earthquake rate increase

Tom Parsons[1] **and Eric L. Geist**[1]

[1]U. S. Geological Survey, Menlo Park, California, USA

Key Points:
- Earthquake rates increased recently
- Increased rates are random
- No evidence for communication above M5.6

Supporting Information:
- Readme
- Figure S1

Correspondence to:
T. Parsons,
tparsons@usgs.gov

Citation:
Parsons, T., and E. L. Geist (2014), The 2010–2014.3 global earthquake rate increase, *Geophys. Res. Lett.*, *41*, 4479–4485, doi:10.1002/2014GL060513.

Received 12 MAY 2014
Accepted 18 JUN 2014
Accepted article online 21 JUN 2014
Published online 3 JUL 2014

Abstract In light of a heightened global earthquake rate during the first quarter of 2014 and recent studies concluding that large earthquakes affect global seismicity for extended periods, we revisit the question whether the temporal distribution of global earthquakes shows clustering beyond that expected from a time-independent Poisson process. We examine a broad window from 1979 to 2014.3 for $M \geq 7.0$ shocks, and a narrow window for $M \geq 5.0$ seismicity since 2010 that has higher than average rates. We test whether a Poisson process can be falsified at 95% confidence to assess the degree of dependent clustering in the catalogs. If aftershocks within at least one rupture length from main shocks/foreshocks are filtered, then we find no evidence of global scale $M \geq 5.2$–5.6 (depending on parameters) clustering since 2010 that demands a physical explanation. There is evidence for interdependence below this threshold that could be a consequence of catalog completeness or a physical process.

1. Introduction

Obvious increases in the global rate of large ($M \geq 7.0$) earthquakes happened after 1992, 2010, and especially during the first quarter of 2014 (Table 1 and Figure 1). Given these high rates, along with suggestions that damaging earthquakes may be causatively linked at global distance [e.g., *Gomberg and Bodin*, 1994; *Pollitz et al.*, 1998; *Tzanis and Makropoulos*, 2002; *Bufe and Perkins*, 2005; *Gonzalez-Huizar et al.*, 2012; *Pollitz et al.*, 2012, 2014], we investigate whether there is a significant departure from a random process underlying these rate changes. Recent studies have demonstrated that $M \geq 7.0$ earthquakes (and also tsunamis) that occurred since 1900 follow a Poisson process [e.g., *Michael*, 2011; *Geist and Parsons*, 2011; *Daub et al.*, 2012; *Shearer and Stark*, 2012; *Parsons and Geist*, 2012; *Ben-Naim et al.*, 2013]. Here we focus on the period since 2010, which has $M \geq 7.0$ rates increased by 65% and $M \geq 5.0$ rates up 32% compared with the 1979–present average. The first quarter of 2014 experienced more than double the average $M \geq 7.0$ rate, enough to intrigue the news media [e.g., http://www.nbcnews.com/science/environment/spike-earthquakes-illusion-raises-new-questions-n85826]. We extend our analysis to $M \geq 5.0$ levels, as many of these lower magnitude events convey significant hazard, and global catalogs have not generally been tested down to these thresholds.

2. Methods and Data

We work with the Advanced National Seismic System (ANSS) catalog of $M \geq 5.0$ global earthquakes for the period between 1979 and 2014.3 with a primary focus on the recent interval between 2010 and 2014.3 that shows the highest earthquake rates (Table 1 and Figure 1). A variety of tests suggest that the catalog is complete down to magnitudes between $M = 4.6$ and $M = 5.2$, depending on the method used to assess it (see supporting information). We examine a range of lower magnitude thresholds above $M = 5.0$ to account for this uncertainty.

We are interested in the question whether the global earthquake rate increase is related to interactions among large events with apparent global reach, or some other broad physical process. We therefore want to remove local aftershocks from the global catalog that can be explained by near-source physics, such as static Coulomb stress change [e.g., *Stein*, 1999]. We identify an exclusion zone around main shocks/foreshocks as a function of rupture length determined from their magnitudes [*Wells and Coppersmith*, 1994]. We use this magnitude-based exclusion of local aftershocks following *Shearer and Stark* [2012], *Tahir et al.* [2012], and *Zakharova et al.* [2013] to enable unequivocal global scale interactions and/or clustering to emerge. We test a variety of radii ($nr = 1$ to $nr = 5$) as $nr \cdot$(rupture length), and a variety of declustering periods from 10 days to 2 years; the vast majority of aftershocks occur in the shorter periods according to Omori's law. We further test a declustered catalog using local main shocks/foreshocks down to the $M \geq 6.0$ level, which is approximately the smallest distance (~12.5 km) we can reasonably apply given location and depth uncertainties. Distance

Table 1. Comparison of the Global Rates of $M \geq 7.0$ and $M \geq 5.0$ Earthquakes During Different Periods Since 1979[a]

	Raw Catalog Rate yr^{-1}		Declustered Rate yr^{-1}	
Period (years)	**M ≥ 5.0**	**M ≥ 7.0**	**M ≥ 5.0**	**M ≥ 7.0**
1979–2014.3 (35.3)	1356.6	10.1	1098.9	7.5
1992–2009 (18)	1352.6	11.6	1060.4	8.7
2010–2014.3 (4.3)	1795.4	16.7	1240.0	10.0
2014–2014.3 (0.3)	1638.4	23.3	1161.1	10.1

[a]The raw catalog rates are given along with a simple declustering that eliminates potential aftershocks that happened within 100 days after, and within one rupture length [*Wells and Coppersmith*, 1994] of $M \geq 6.0$ potential foreshocks/main shocks.

ranges between main shocks and possibly triggered events are calculated with the inverse method of *Vincenty* [1975], using the NAD83 ellipsoid.

We step through declustered catalogs at regular intervals and calculate differences in the number of earthquakes in symmetrical periods, such as the changes over ±48 h in $M \geq 5.0$ seismicity shown in Figure 2. For reference, we compare these changes with those associated with global $M \geq 7$ main shocks because this has been suggested as an important effect in the example of the 2012 $M = 8.6$ Indian Ocean earthquake [*Pollitz et al.*, 2012, 2014]. We map out some of these larger rate changes to gain insight into their spatial character for comparison purposes in Figures 2 and 3. For statistical tests we primarily work with binned earthquake count data, like the $M \geq 7.0$ catalogs in Figure 1.

The key question we address is whether there is evidence for systematic (nonrandom) large earthquake clustering at global scale that requires a physical explanation. We therefore calculate the fit of earthquake occurrence in different bin widths (1–5 days for $M \geq 5.0$ events) to Poisson and negative binomial counts to identify dependent clustering [e.g., *Vere-Jones*, 1970; *Jackson and Kagan*, 1999]. By "dependent clustering" we mean that events concentrate in time and/or are separated by quiet intervals to degrees not expected by random chance. Local aftershock sequences are an example of dependent temporal and spatial concentration. A statistical indication that a Poisson process cannot describe the observations at high confidence occurs when the data are overdispersed, with a variance greater than the mean (μ) as $var = \mu + \alpha\mu^2$, where α is the dispersion parameter ($\alpha = 0$ for a Poisson process). Overdispersion is the presence of greater variability than would be expected based on a simple statistical model (Poisson process in this case) and an indication of time dependence between earthquakes. Identifying significant overdispersion does not in itself prove that the observations are most consistent with a negative binomial distribution, but rather that they are not independently distributed [e.g., *Luen and Stark*, 2012].

We apply a maximum likelihood regression technique [*Cameron and Trivedi*, 1998] that starts with fitting a Poisson model, then a null model (intercept only model), and finally the negative binomial model. We iterate until the increase in the log likelihood is vanishingly small. We estimate the dispersion (α) inherent to each catalog from the maximum likelihood regressions. We test the significance of non-zero α values by calculating the likelihood ratio as

$$LR = -2 \ln \left[\frac{\ell_{Poisson(\alpha=0)}}{\ell_{negative\_binomial(\alpha>0)}} \right].$$

Likelihood ratio values less than 2.705 (critical value for 95% confidence associated with the χ^2-distribution) imply that a Poisson process cannot be ruled out [*Gutierrez et al.*, 2001; *Hilbe*, 2011].

3. Results

We reproduce prior results showing a lack of temporal dependence amongst annually binned $M \geq 7.0$ earthquakes [*Michael*, 2011; *Geist and Parsons*, 2011; *Daub et al.*, 2012; *Shearer and Stark*, 2012; *Parsons and Geist*, 2012] and, provided that the data are declustered in near source areas, extend them through 2014.3 (Figure 1). The probability of a Poisson process is ~24% if the 1979–2014.3 $M \geq 7.0$ catalog is declustered following $M \geq 7.0$ main shocks, and is ~100% if declustering after $M \geq 6.0$ foreshocks is conducted.

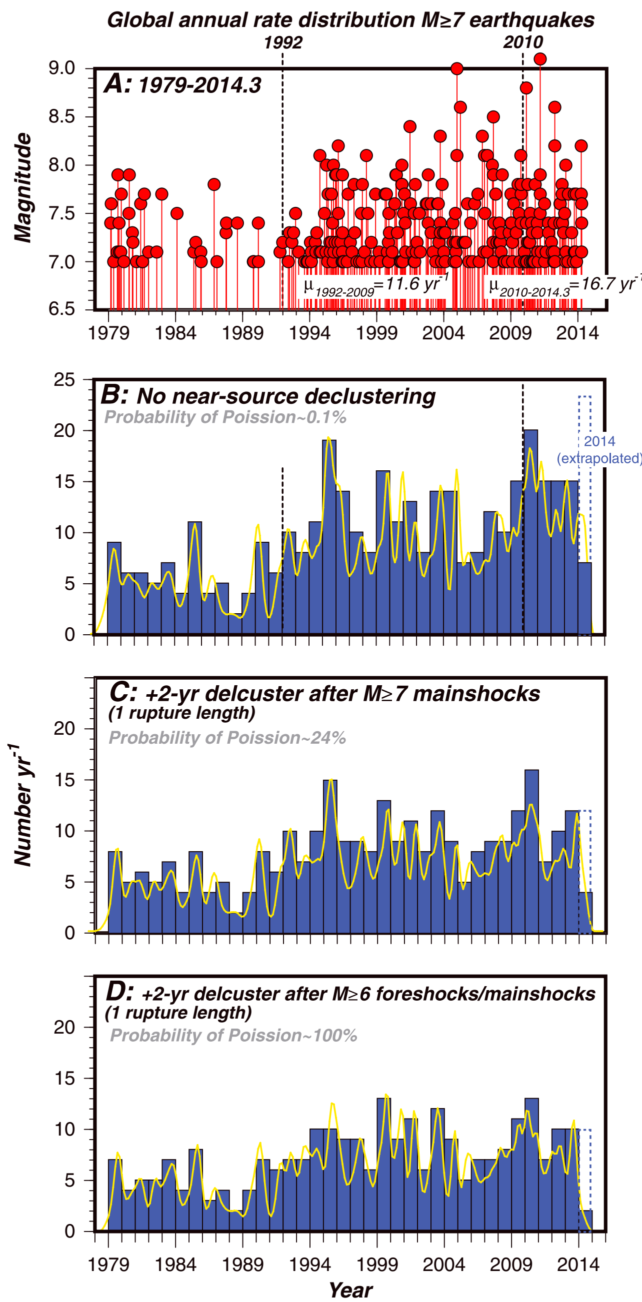

Figure 1. Temporal global distribution of $M \geq 7.0$ earthquakes since 1979. The average rate over this period is 10.1 yr^{-1}. In Figure 1a a clear rate increase is evident after ~1992, with the average increasing to 12.5 yr^{-1}. Since 2010 the rate has increased to 16.7 yr^{-1}. In Figure 1b the catalog of Figure 1a is expressed as an annual histogram (blue columns) as well as a kernel density plot (yellow curve) with variable width [*Salgado-Ugarte and Perez-Hernandez*, 2003]. The purpose of the kernel density plot is to illustrate the effects of a histogram representation of the data. This catalog is not random in time and cannot be fit to a Poisson distribution; the data exhibit overdispersion likely because of dependent clustering (local aftershocks). In Figure 1c the catalog is declustered by removing earthquakes that occurred within 2 years time, and one rupture length [*Wells and Coppersmith*, 1994] away from $M \geq 7.0$ main shocks. A Poisson distribution cannot be falsified at 95% confidence for this catalog. In Figure 1d the same process is followed except that declustering is conducted with $M \geq 6.0$ foreshocks/main shocks, and $M \geq 7.0$ earthquakes that occurred within 2 years time, and one rupture length away are removed. After that process, the probability that the catalog origin times are independent is ~100%.

10.1002/2014GL060513

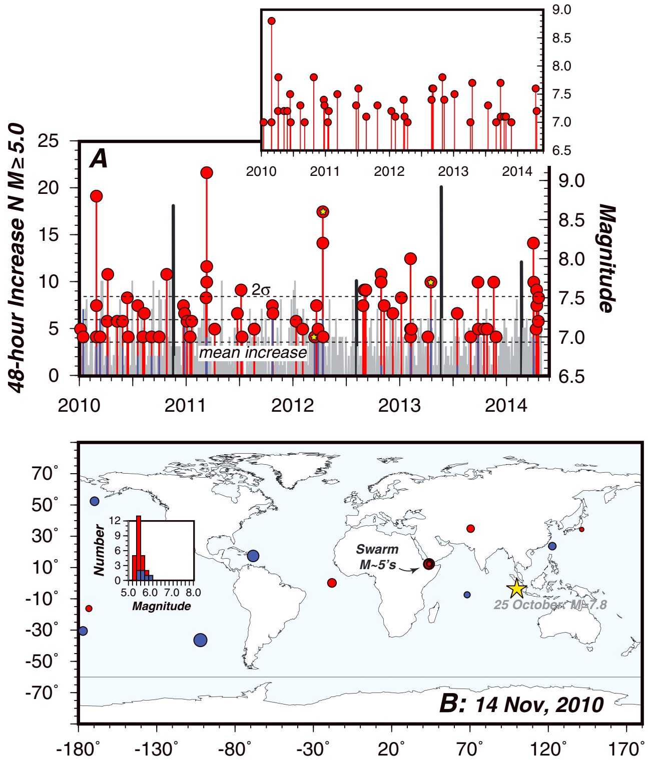

Figure 2. Focus on 2010–2014.4 seismicity rates. The purpose of this figure is to explore possible global-level earthquake communications. (a) $M \geq 7.0$ events are plotted against time and magnitude (red stick plot). A declustered version (Figure 1d) is shown in the inset. $M \geq 5.0 \pm 48$ h rate increases are plotted as gray lines, and those that can be temporally associated with $M \geq 7.0$ global main shocks are shaded blue. Local aftershocks within one rupture length from $M \geq 6.0$ earthquakes are removed from the $M \geq 5.0$ catalog. Generally, $M \geq 5.0$ rate increases are as likely to occur independently as they are to be associated in time with global main shocks. The greatest $M \geq 5.0$ rate increases are not temporally associated with global $M \geq 7.0$ main shocks. Stars indicate main shocks mapped in Figures 3d–3f. In Figure 2b, the largest increase ($\Delta r = 18$) in 2010 is mapped (spike is shown with a heavy black line in Figure 2a). The other black lines correspond to mapping in Figures 3a–3c. Red circles show the succeeding 48 h of $M \geq 5.0$ seismicity, and blue circles plot events from the preceding 48 h period. A swarm of $M \sim 5$ events in the Afar region is responsible for the rate increase. The global main shock ($M = 7.8$) closest in time occurred 20 days previously in Indonesia (yellow star).

We extend the analysis to $M \geq 5.0$ for the 2010–2014.3 period and systematically vary parameters. These include lower magnitude threshold (0.1 magnitude unit steps), binning width for earthquake counts (1–5 days), number of rupture lengths within which to exclude local aftershocks (1–5), and aftershock duration (10–100 days). The resulting 2500 histograms are then tested to see if a Poisson null hypothesis can be falsified and the likelihood ratio (*LR*) test for dispersion parameter $\alpha = 0$ is reported for each histogram. If a Poisson process can be falsified at 95% confidence ($LR > 2.705$) [*Gutierrez et al.*, 2001; *Hilbe*, 2011], then we conclude that there is dependent clustering associated with the catalog [e.g., *Vere-Jones*, 1970; *Jackson and Kagan*, 1999]. Results from these calculations are plotted in Figure 4.

The three most influential factors that control whether a catalog shows global-scale clustering behavior vs. whether events are independent in time are: (1) near-source declustering, (2) binning, and (3) the lower magnitude threshold examined. These parameters are isolated in the plots of Figure 4. All catalogs are overdispersed if no local aftershocks are removed, which is an expected result [*Kagan*, 2010]. Removing events within one rupture length of $M \geq 6.0$ main shocks/foreshocks for just the first 10 days causes all catalogs above $M = 5.6$ to be consistent with a Poisson process at any of the binning widths we test.

Of course the number of events in our catalogs decreases with increasing the lower magnitude threshold, so we are curious if the smaller sample size might make the catalogs appear to be more independent. To assess this we randomly subsample a known dispersive catalog, the 2010–2014.3 $M \geq 5.0$ catalog declustered at one rupture length and 100 days (Figure 4). The initial catalog has 5333 events; we select 869 of these at random, which is the number of $M \geq 5.7$ events in the catalog. We do this 100 times, bin them at 2 days, and test to see if they retain the dispersive character of their parent distribution. The results are plotted in Figure 4c; all 100 subsampled catalogs are significantly overdispersed, and it thus does not seem that the smaller sampling is responsible for the independent temporal distribution above $M = 5.6$. The lower magnitude threshold studied was also noted to influence consistency with a Poisson process by *Daub et al.* [2012] and *Luen and Stark* [2012] for global and Southern California catalogs, respectively; both studies suggest that accuracy issues with magnitude and location determination might influence this.

An additional feature that we note in the global catalogs is swarms of events around the $M \sim 5$ level, something that is comparatively rare at higher magnitudes [e.g., *Sykes*, 1970; *Ibs-von Seht et al.*, 2008]. An

10.1002/2014GL060513

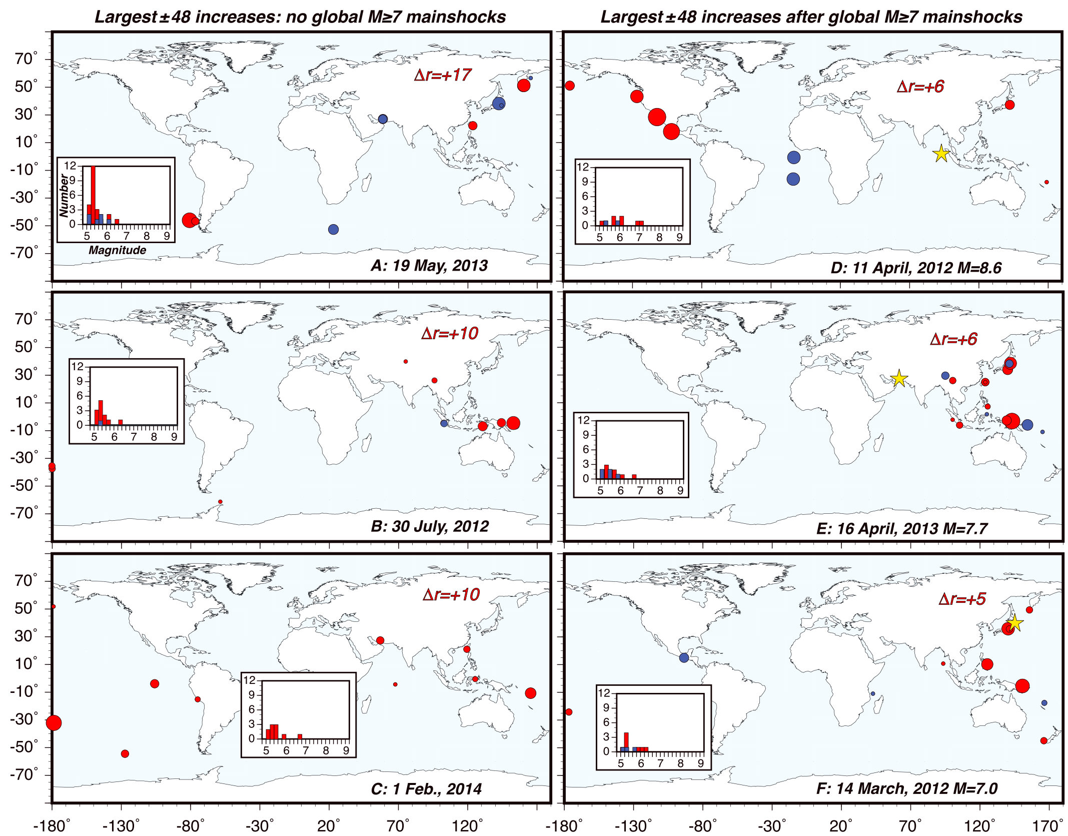

Figure 3. Mapping of the largest 2010–2014.4 $M \geq 5.0$ seismicity rate increases that (a–c) are not associated with global $M > 7.0$ main shocks (black lines in Figure 2a), and (d–f) those that occurred within 48 h of global $M \geq 7.0$ main shocks (yellow stars show epicenters; also displayed in Figure 2a). Red and blue dots show $M \geq 5.0$ events 48 h after and before respectively. The purpose of the figure is to demonstrate that random 48 h periods can have spatial seismicity outbreaks that compare with those associated with global main shocks. Histograms show magnitude distributions of plotted earthquakes.

example is plotted in Figure 2b, where 18 $5.0 \leq M \leq 5.2$ earthquakes occurred in the Afar region of Africa in a 48 h period, and there is no local or global main shock associated with them. The events are likely related to active magmatism, and this sort of clustering is not removed in our analysis. To test the role of swarms on our results, we decluster using $M \geq 5.0$ foreshocks at five rupture lengths and 100 days, which removes all swarms from the catalog. The likelihood ratio test from this experiment yields a value of 19.1, exceeding the critical χ^2-distribution 95% confidence value of 2.705, and implying a ~0% probability of a Poisson process. There thus may be dependent clustering below the $M \sim 5.2$ to $M \sim 5.6$ level, which defines our resolution on the threshold (Figure 4). Unless the post-2010 catalog is incomplete below $M \sim 5.2$ to $M \sim 5.6$, or there are significant magnitude assignment and/or location errors, this means that global scale interactions or some other physical process like tidal stressing [e.g., *Cochran et al.*, 2004; *Tanaka*, 2012] may be significant below these magnitude thresholds. Long range dynamic triggering of $M \leq 5.2$–$M \leq 5.6$ earthquakes could be an explanation, as this magnitude range is near the threshold where significant rate increases are associated with global main shocks (Figure 2) [*Huc and Main*, 2003; *Velasco et al.*, 2008; *Parsons and Velasco*, 2011; *Peng et al.*, 2010, 2011; *Gonzalez-Huizar et al.*, 2012; *Parsons et al.*, 2014].

4. Conclusions

A strong increase in the number of global earthquakes is noted since 2010 that appears to have accelerated during the first quarter of 2014. However, there is no evidence that this increase represents a departure from temporally independent earthquake occurrence, as many of these earthquakes are local aftershocks of prior events. While some studies have concluded that specific large earthquakes have had a significant impact on

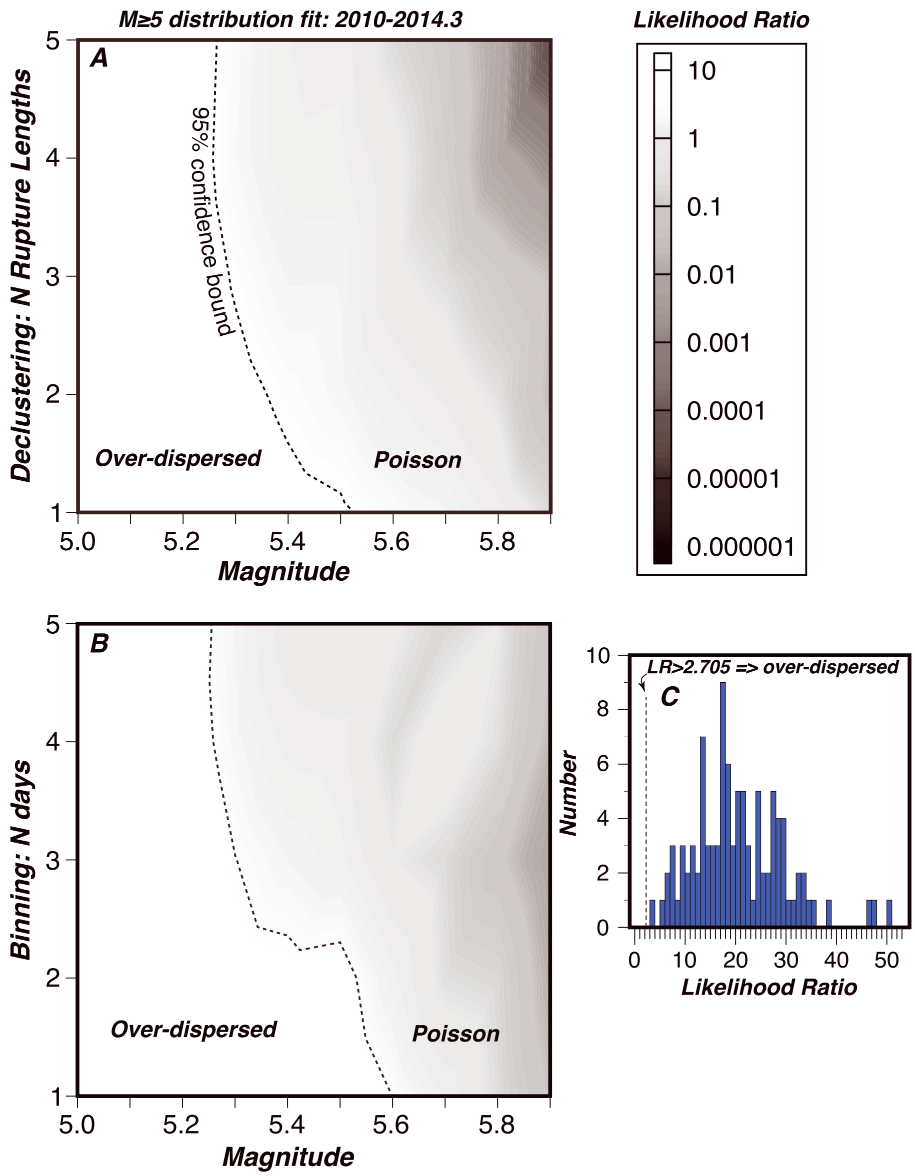

Figure 4. Likelihood ratio tests for Poisson ($\alpha = 0$) null hypothesis. Values greater than 2.705 indicate significant overdispersion (clustering), implying that a Poisson process cannot be established with 95% confidence [*Gutierrez et al*., 2001; *Hilbe*, 2011]. Results are plotted against lower magnitude threshold along with (a) declustering parameter (number main shock rupture lengths), and (b) binning. It appears from these plots that higher magnitude ($M \geq 5.6$) events are independently distributed, whereas lower magnitude events show clustering. However the number of higher magnitude events is also lower. In Figure 4c 100 catalogs are drawn at random from the declustered 2010–2014.4 $M \geq 5.0$ catalog (5333 events) that is overdispersed. Each randomly drawn catalog has 869 events, which corresponds to the number of $M \geq 5.7$ shocks. The histogram shows 100 likelihood ratio tests for $\alpha = 0$ (Poisson), which are all greater than 2.705, and are thus are rejected. Therefore the change from an overdispersed, clustered catalog to an independently distributed one at higher magnitudes is not the result of a smaller sample size.

global $M \geq 5.0$ seismicity since 2010, we cannot find a strong signal associated with global $M \geq 7.0$ earthquakes that rises above the random fluctuations that are observed between regular 48 h periods; the largest rate increases we see are not associated with global main shocks (Figure 2). This is quantified here at the $M \geq 5.6$ level because a temporally independent Poisson process governing the distribution of these earthquakes cannot be ruled out at 95% confidence, even with a wide range of local declustering and binning parameters. If $M \geq 7.0$ earthquakes have significant global influence on other moderate to large events ($M \geq 5.6$), then the catalog should be overdispersed well outside local aftershock zones. We do note apparent dependent clustering below this magnitude threshold that cannot be explained by local aftershocks or swarms.

Acknowledgments
We thank Editor Andrew Newman, and two anonymous reviewers for constructive comments. We accessed the Advanced National Seismic System catalog data through the Northern California Earthquake Data Center site at: http://quake.geo.berkeley.edu/anss/catalog-search.html.

The Editor thanks Richard Aster and an anonymous reviewer for their assistance in evaluating this paper.

References

Ben-Naim, E., E. G. Daub, and P. A. Johnson (2013), Recurrence Statistics of Great Earthquakes, *Geophys. Res. Lett.*, *40*, 3021–3025, doi:10.1002/grl.50605.

Bufe, C. G., and D. M. Perkins (2005), Evidence for a Global Seismic-Moment Release Sequence, *Bull. Seismol. Soc. Am.*, *95*, 833–843, doi:10.1785/0120040110.

Cameron, A. C., and P. K. Trivedi (1998), *Regression Analysis of Count Data*, 411 pp., Cambridge Univ. Press, New York.

Cochran, E. S., J. E. Vidale, and S. Tanaka (2004), Earth tides can trigger shallow thrust fault earthquakes, *Science*, *306*(5699), 1164–1166.

Daub, E., E. Ben-Naim, R. Guyer, and P. Johnson (2012), Are mega-quakes clustered?, *Geophys. Res. Lett.*, *39*, L06308, doi:10.1029/2012GL051465.

Geist, E. L., and T. Parsons (2011), Assessing historical rate changes in global tsunami occurrence, *Geophys. J. Int.*, *187*, 497–509, doi:10.1111/j.1365-246X.2011.05160.x.

Gomberg, J., and P. Bodin (1994), Triggering of the $Ms = 5.4$ Little Skull Mountain, Nevada, earthquake with dynamic strains, *Bull. Seismol. Soc. Am.*, *84*(3), 844–853.

Gonzalez-Huizar, H., A. A. Velasco, Z. Peng, and R. R. Castro (2012), Remote triggered seismicity caused by the 2011, M9.0 Tohoku-Oki, Japan earthquake, *Geophys. Res. Lett.*, *39*, L10302, doi:10.1029/2012GL051015.

Gutierrez, R. G., S. Carter, and D. M. Drukker (2001), On boundary-value likelihood-ratio tests, *Stat. Tech. Bull.*, *60*, 15–18.

Hilbe, J. M. (2011), *Negative Binomial Regression*, 2nd ed., 576 pp., Cambridge Univ. Press, New York.

Huc, M., and I. G. Main (2003), Anomalous stress diffusion in earthquake triggering: Correlation length, time dependence, and directionality, *J. Geophys. Res.*, *108*(B7), 2324, doi:10.1029/2001JB001645.

Ibs-von Seht, M., T. Plenefisch, and K. Klinge (2008), Earthquake swarms in continental rifts - A comparison of selected cases in America, Africa and Europe, *Tectonophysics*, *452*, 66–77, doi:10.1016/j.tecto.2008.02.008.

Jackson, D. D., and Y. Y. Kagan (1999), Testable earthquake forecasts for 1999, *Seism. Res. Lett.*, *70*, 393–403.

Kagan, Y. Y. (2010), Statistical distributions of earthquake numbers: Consequence of branching process, *Geophys. J. Int.*, *180*, 1313–1328.

Luen, B., and P. B. Stark (2012), Poisson tests of declustered catalogues, *Geophys. J. Int.*, *189*, 691–700, doi:10.1111/j.1365-246X.2012.05400.x.

Michael, A. J. (2011), Random variability explains apparent global clustering of large earthquakes, *Geophys. Res. Lett.*, *38*, L21301, doi:10.1029/2011GL049443.

Parsons, T., and E. L. Geist (2012), Were global $M \geq 8.3$ earthquake time intervals random between 1900-2011?, *Bull. Seismol. Soc. Am.*, *102*, 1583–1592, doi:10.1785/01201100282.

Parsons, T., and A. A. Velasco (2011), Absence of remotely triggered large earthquakes beyond the main shock region, *Nat. Geosci.*, *4*, 312–316, doi:10.1038/ngeo1110.

Parsons, T., M. Segou, and W. Marzocchi (2014), The global aftershock zone, *Tectonophysics*, *618*, 1–34, doi:10.1016/j.tecto.2014.01.038.

Peng, Z., D. P. Hill, D. R. Shelly, and C. Aiken (2010), Remotely triggered microearthquakes and tremor in central California following the 2010 Mw 8.8 Chile earthquake, *Geophys. Res. Lett.*, *37*, L24312, doi:10.1029/2010GL045462.

Peng, Z., C. Wu, and C. Aiken (2011), Delayed triggering of microearthquakes by multiple surface waves circling the Earth, *Geophys. Res. Lett.*, *38*, L04306, doi:10.1029/2010GL046373.

Pollitz, F. F., R. Burgmann, and B. Romanowicz (1998), Viscosity of oceanic asthenosphere inferred from remote triggering of earthquakes, *Science*, *280*, 1245–1249.

Pollitz, F. F., R. S. Stein, V. Sevilgen, and R. Bürgmann (2012), The 11 April 2012 east Indian Ocean earthquake triggered large aftershocks worldwide, *Nature*, *490*(7419), 250–253.

Pollitz, F. F., R. Bürgmann, R. S. Stein, and V. Sevilgen (2014), The profound reach of the 11 April 2012 M 8.6 Indian Ocean earthquake: Short-term global triggering followed by a longer-term global shadow, *Bull. Seismol. Soc. Am.*, *104*, 972–984, doi:10.1785/0120130078.

Salgado-Ugarte, I. H., and M. A. Perez-Hernandez (2003), Exploring the use of variable bandwidth kernel density estimators, *Stat. J.*, *3*(2), 133–147.

Shearer, P. M., and P. B. Stark (2012), The global risk of big earthquakes has not recently increased, *Proc. Natl. Acad. Sci. U.S.A.*, *109*, 717–721, doi:10.1073/pnas.1118525109.

Stein, R. S. (1999), The role of stress transfer in earthquake occurrence, *Nature*, *402*, 605–609.

Sykes, L. R. (1970), Earthquake swarms and sea-floor spreading, *J. Geophys. Res.*, *75*, 6598–6611, doi:10.1029/JB075i032p06598.

Tahir, M., J.-R. Grasso, and D. Amorèse (2012), The largest aftershock: How strong, how far away, how delayed?, *Geophys. Res. Lett.*, *39*, L04301, doi:10.1029/2011GL050604.

Tanaka, S. (2012), Tidal triggering of earthquakes prior to the 2011 Tohoku-Oki earthquake (Mw 9.1), *Geophys. Res. Lett.*, *39*, L00G26, doi:10.1029/2012gl051179.

Tzanis, A., and K. Makropoulos (2002), Did the 7/9/1999 M5.9 Athens earthquake come with a warning?, *Nat. Hazards*, *27*(1–2), 85–103, doi:10.1023/A:1019957228371.

Velasco, A. A., S. Hernandez, T. Parsons, and K. Pankow (2008), Global ubiquity of dynamic earthquake triggering, *Nat. Geosci.*, *1*, 375–379, doi:10.1038/ngeo204.

Vere-Jones, D. (1970), Stochastic models for earthquake occurrence (with discussion), *J. R. stat. Soc.*, *B32*, 1–62.

Vincenty, T. (1975), Direct and inverse solutions of geodesics on the ellipsoid with application of nested equations, *Surv. Rev.*, *XXII*(176), 88–93.

Wells, D. L., and K. J. Coppersmith (1994), New empirical relationships among magnitude, rupture length, rupture width, rupture area, and surface displacement, *Bull. Seismol. Soc. Am.*, *84*, 974–1002.

Zakharova, O., S. Hainzl, and C. Bach (2013), Seismic moment ratio of aftershocks with respect to main shocks, *J. Geophys. Res. Solid Earth*, *118*, 5856–5864, doi:10.1002/2013JB010191.